

Double electron removal and fragmentation model of the H_2 molecule by highly charged ions

C. J. Wood and R. E. Olson

Department of Physics, University of Missouri–Rolla, Rolla, Missouri 65401

(Received 26 May 1998)

A five-body classical trajectory Monte Carlo model has been developed to study double electron removal from H_2 by collisions with highly charged ions at impact energies ranging from 1 eV/u to 1 GeV/u. The longitudinal and transverse final-state correlation between ejected electrons is calculated for double ionization of H_2 by impact of Se^{28+} at 3.6 MeV/u and U^{92+} at 1 GeV/u; the electron-electron interaction is dynamically included during the collision when one of the electron's total energy becomes positive. Relativistic corrections are incorporated to reflect the Lorentz contraction of the projectile's electric field. The cross section dependence on the alignment of the H_2 molecular axis was investigated. Here, transfer ionization of H_2 by O^{8+} at 500 keV/u is found to have a maximum for the molecular axis aligned perpendicular to the projectile velocity, while no orientation dependence is found for double ionization at 500 keV/u. In contrast, a minimum in the cross section at 90° is found for 1-GeV/u $U^{92+}+H_2$ collisions. A systematic study of the energy partitioning between the two product H^+ ions has been made for $Xe^{54+}+H_2$ from 1 eV/u to 1 MeV/u. Large deviations from Franck-Condon behavior are found for impact energies $E \lesssim 10$ keV/u. At low energies the proton energies are very energetic with the main contribution arising from collisional transfer from the projectile, while the proton energy spectrum at high impact energy is due to the Coulomb explosion of the isolated molecule. [S1050-2947(99)07502-2]

PACS number(s): 34.10.+x, 34.50.-s

I. INTRODUCTION

The removal of two electrons from an atom or molecule by the interaction of a heavy, highly charged ion can lead to double ionization, transfer ionization, or double electron capture reactions. Double ionization of a target such as He or H_2 by a fast, heavy ion will lead to correlated motion between the ejected electrons and the projectile and recoil ions. The study of ion-molecule reactions leads to the further complication of the dependence on the alignment of the molecular axis. In addition, double electron removal from H_2 results in dissociation of the molecule and the subsequent Coulomb explosion of the protons. For a sufficiently slow ion, the correlation in the postcollision regime will be a five-body problem that includes three heavy particles, all with approximately equivalent speeds.

Analysis of final-state energies and momenta of the collision products gives insight into the dynamics of the capture and ionization removal mechanisms. This has been achieved for atomic targets experimentally through the development of recoil-ion momentum spectroscopy [1] with the coincident detection of low energy electrons [2,3]. Moshhammer *et al.* [4,5] have performed extensive measurements for $Se^{28+}+He$ single and double ionization at 3.6 MeV/u. For the double-ionization channel, they have found that the longitudinal momentum balance between the recoil ion and the sum momentum of the ionized electrons ($\Sigma P_{e\parallel}$) is the result of the correlated motion of the initially bound electrons [4]. The work also showed that electrons are mainly emitted with positive longitudinal momentum due to a strong postcollision interaction with the projectile. Electron-electron correlation was also displayed with one electron moving slowly and the other moving comparatively fast. Classical trajectory Monte Carlo (CTMC) calculations, which included the electron-electron interaction in the postcollision regime, showed good

agreement with the longitudinal momenta spectra, and qualitative agreement with the observed electron-electron correlation.

The single-ionization channel for this system ($Se^{28+}+He$) has also been studied in a kinematically complete experiment [5] and in a work by Olson *et al.* [6]. Analysis of momentum spectra for this system relied upon a collision plane defined by the incoming projectile momentum and the final transverse momentum of the recoil ion. This collision plane has been used by other workers in the field [7–9] to display final-state momenta spectra of ion-atom collisions and to identify signatures of various ionization mechanisms. In this notation the projectile's incident momentum defines the $+z$, or longitudinal direction. The x and y components are in the plane perpendicular to the longitudinal vector.

In a recent paper by Wood *et al.* [10], CTMC calculations for single and double ionization of He by 1-GeV/u U^{92+} ions displayed a significant reduction in the projectile postcollision interaction due to relativistic corrections to the projectile interaction. This leads to the longitudinal electron spectra being nearly symmetric about $P_{e\parallel}=0$. The electron correlation found in double-ionization events is similar to that observed for collisions with 3.6-MeV/u Se^{28+} ions. However, the lack of the postcollision interaction (PCI) from the projectile allows the correlation between the electrons to be seen more clearly. The calculations indicated that electron-electron interactions in the postcollision regime are needed to properly describe the electron momenta spectra. In addition, Keller *et al.* [11] used the Weizsäcker-Williams equivalent photon method to conclude that both initial-state and postcollision correlation are needed to fully understand the electron-electron interactions.

In the systems described above, electron correlation for the double-ionization reaction was examined in only the longitudinal direction. The electron correlation, if any, in the transverse plane has yet to be explored experimentally or

theoretically. By expanding on the previous methods of analysis, our work will explore the transverse electron correlation in 3.6-MeV/u $\text{Se}^{28+} + \text{H}_2$ and 1-GeV/u $\text{U}^{92+} + \text{H}_2$ double-ionization collisions using the CTMC method. The longitudinal electron correlation will also be presented to compare to previous studies on double ionization of He. By doing this, the H_2 model will be tested and any variations in electron spectra due to the different targets may be determined. These differences may include the ejected electrons scattering off one of the molecular target atoms in a secondary collision, and redistribution of the momentum due to the Coulomb explosion of the molecule.

Along with the development of recoil-ion-momentum spectroscopy, recent progress has been made in the field of ion-molecule scattering. The coincidence time-of-flight technique has made it possible to measure the dissociation channels for highly ionized molecular ions [12–14]. These procedures make it possible to explore possible orientation effects of different ionization channels in ion-molecule collisions. Recent experimental reports have focused on the orientation dependence of double ionization and transfer ionization of diatomic molecules by electrons and heavy ions. Double ionization of H_2 by 1-MeV/u electrons displays a maximum at 0° to the beam direction [15,16], while the study shows the distribution is nearly isotropic for proton impact at 1 MeV/u. The lack of dependence on the orientation of the molecular axis for double ionization, for heavy-ion projectiles, was also observed in $\text{O}^{8+} + \text{D}_2$ at impact energies ranging from 0.125 MeV/u to 1 MeV/u [14]. In contrast, transfer ionization and transfer excitation of D_2 by O^{8+} impacting at 0.125–1 MeV/u show maxima at 90° for energies greater than 0.125 MeV/u. This anisotropy has been attributed to interference between the two atomic centers. A theoretical work on electron capture [17] using the continuum-distorted-wave-eikonal-final-state model for $\text{O}^{8+} + \text{H}_2$ at 625 keV/u supported the experimental data of Cheng *et al.* [14]. In a recent work, Wohrer and Watson [18] have used a geometrical argument within the independent-electron approximation to conclude that geometrical effects on the ionization cross sections for H_2 should be small. In our work an attempt will be made to determine if any part of the orientation dependence can be attributed to classical scattering processes.

In a double electron removal process from molecular hydrogen, the target protons attain energy via transfer of energy from the projectile and from the kinetic energy released during the dissociation. The collisional energy transfer decreases as the impact energy increases, and the kinetic energy released is determined by the Franck-Condon transition to the Coulomb potential of the two protons. Knowledge of the proton kinetic energy will be helpful in understanding the low energy collision cross sections such as those observed by Beck *et al.* [19] at the electron beam ion trap (EBIT) at Livermore. In these measurements, double capture from H_2 by highly charged ions shows the ratio of double to single capture cross sections for projectile charges $q > 35$ to be approximately 30%.

If the projectile has a velocity near the final speed of the target protons, then interesting energy sharing will result. For example, a high degree of correlated motion has been revealed by Wiese *et al.* [20] for $\text{H}^- + \text{H}_2$ dissociative collisions.

In our present work, we will focus on the energy and momentum spectra of the target protons produced by double electron removal due to Xe^{54+} ion impact at energies ranging from 1 eV/u to 1 MeV/u. Such collisions are mediated by double electron capture at low energies, transfer ionization at intermediate energies, and double ionization at high energies.

II. THEORY

The classical trajectory Monte Carlo method for ion-atom collisions has been thoroughly described in previous papers [21–24]. Briefly, random numbers that are constrained by Kepler's equation are used to initialize the plane and eccentricity of each electron's orbit. Another random number is used to determine the impact parameter within the range of interaction. Then, a fourth-order Runge-Kutta integration method is applied to solve the first-order, coupled differential equations arising from Hamilton's method. The Runge-Kutta integration is suitable because of its ease of use and its ability to vary the time step. This latter requirement is essential since it is not uncommon for the time step to vary by three orders of magnitude during a single trajectory. Aspects important to the success of the method are good approximations of the quantum mechanical ground-state radial and momentum distributions of the target atom and inclusion of interactions between all particles. Recent enhancements to the CTMC method include the addition of the electron-electron Coulomb interaction [4,10] in the postcollision regime, and the contracted field of a relativistic projectile [10]. In this work, both of these enhancements will be incorporated into a five-body model for H_2 targets.

The model for ion-molecule collisions using the CTMC method is generally the same as for atomic targets, described in [21–24], with the exception that an additional target center is involved. This increases the complexity to a five-body problem. In describing the system, a practical scheme to treat the bound electrons and the atomic centers must be used. Previous CTMC studies on H_2 targets have used independent-electron models with a single electron [25] to calculate ionization and capture by heavy ions. The continuum-distorted-wave-eikonal-final-state (CDW-EFS) model has been used within a two independent center approximation to study single electron capture [17].

In our work two atomic centers, each with one electron, are used to enable the direct investigation of double electron removal mechanisms from H_2 . The Hamiltonian for the five-body system is

$$H = \sum_{i=1}^5 \frac{p_i^2}{2m_i} + \sum_{i=1}^4 \sum_{j=i+1}^5 V_{ij}, \quad (1)$$

where p_i is the momentum of a given particle, m_i a particle's mass, r_{ij} is the distance between i and j , and V_{ij} is the potential between i and j . A desirable treatment would have the potential terms as pairwise Coulomb interactions

$$V(r_{ij}) = \frac{Z_i Z_j}{r_{ij}} \quad (2)$$

throughout the collision process. This is acceptable for the projectile-electron, projectile-target, and electron-parent-

nucleus interactions. However, using Eq. (2) for the electron-electron, and electron–other-target-nucleus terms causes instability in the classical initial state. To overcome this problem, the initial state of the molecule is modeled by two independent hydrogen atoms. Each electron will be initially bound to its parent atomic center by the Coulomb force, and have no dependence on the other atomic center or the other electron. The two atom molecule is held together by a Morse potential [26]

$$V_m(R) = D_e(1 - e^{-\beta_e(R - r_e)})^2, \quad (3)$$

where D_e is the dissociation energy, R is the separation of the atomic centers, and r_e is the separation defined such that $V_m(r_e)$ is a minimum. The values for $D_e = 4.7$ eV, $r_e = 1.40$ a.u., and the curvature parameter $\beta_e = 0.73$ a.u. are determined from spectroscopic data [26]. With the implementation of the Morse interaction, the collisional dissociation of an isolated H_2 molecule to its ground-state atoms is theoretically well described.

The CTMC is a statistical method, so thousands of trajectories must be calculated to ensure small statistical errors. As previously described [21–24], the initial state of each trajectory is selected by randomly generating the position and momentum of the particles in the system. To extend the method to the H_2 molecule, additional random quantities must be generated for the position and momentum of both atomic centers. It is assumed that the molecule is in the ground vibrational state with a separation distance selected randomly from its vibrational Gaussian squared distribution centered about the minimum of the potential well ($r_e = 1.40$ a.u.) of the Morse potential, Eq. (3). This vibrational distribution is necessary to obtain the correct Franck-Condon energy distribution of the dissociating protons for the isolated molecule. The momentum in the center-of-mass frame is calculated by

$$P_{c.m.} = \sqrt{2\mu E_v - V_m(R)}, \quad (4)$$

where μ is the reduced mass of the two atoms and E_v is the vibrational ground-state energy. The momenta of the individual atoms are

$$p_H = \pm \frac{P_{c.m.}}{2}, \quad (5)$$

with the atoms moving along a line towards or away from each other. The intermolecular axis is then rotated into a randomly generated orientation. The electrons are placed on the atoms as described for this simple hydrogenic case in [22], with the ionization potential for each electron set equal to 15.6 eV, the vertical transition from the ground vibrational state of H_2 to that of H_2^+ , see Fig. 1.

As the system is classically evolved and one or both electrons are removed from the molecule during the collision, interactions are included to replicate the potential curves of H_2 and its ions, Fig. 1. To dynamically model the interactions between isolated H_2 and its ions, if one electron attains a positive energy during the collision, represented by the H_2^+ curve of Fig. 1, the Coulomb electron-electron interaction is included in the Hamiltonian along with the Coulomb interactions between both electrons and all atomic centers. Since the coupled equations are stiff, we used a switching

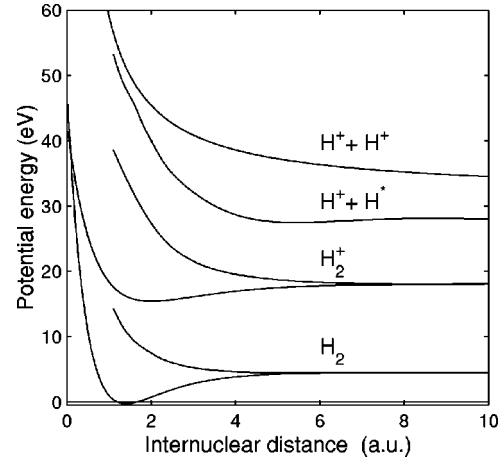


FIG. 1. Schematic of the H_2 , H_2^+ , and $H^+ + H$ potential energies.

function defined by $1 - \exp(-\alpha E_i)$, where $\alpha = 5$ and E_i is the positive energy of the electron with respect to its transition point. If the electron remaining on the molecule reaches an energy corresponding to the first excited state, $H^*(n = 2)$, the Morse potential between the two centers is slowly switched off and the potential curve for H_2^{+*} becomes Coulombic. This simulates the $H^+ + H^*$ dissociating interactions which are molecular Rydbergs of $H^+ + H^+$ for $R < 5$ a.u. For complete double electron removal, the Hamiltonian then becomes a five-body Coulomb problem. Double electron removal will place the system in a repulsive state, labeled as $H^+ + H^+$, in Fig. 1. Since all interactions are included in the final state, the momenta of each particle can be determined to produce a kinematically complete calculation for the double electron removal process.

It is important to note that the energy required to remove both electrons from H_2 is the sum of the ionization energies for the two electrons 31.2 eV, the 4.7 eV needed to break the ground-state H_2 molecular bond, and the approximately 19 eV required to place the two protons on the repulsive Coulomb curve at the equilibrium separation. Our model overestimates the true energy required to remove both electrons in a vertical Franck-Condon transition by 4 eV (54.9 eV instead of 50.9 eV) because of our desire to have the flux lost to single electron removal properly portrayed. If the H_2 molecule is displaced from its equilibrium position during the collision, the corresponding energy required for double electron removal will differ from the vertical Franck-Condon transition and be portrayed by the changes of the Morse interaction and the internuclear position of fragmentation on the repulsive $H^+ + H^+$ Coulomb curve.

In order to extend the CTMC model to relativistic heavy ions, the potential due to the projectile must be modified to account for the contraction of the electric field. It is assumed that the projectile is the only particle with a relativistic velocity and time retardation is ignored. The field due to the projectile has the form [10]

$$\mathbf{E} = \frac{Z_p \mathbf{r}}{r^3 \gamma^2 (1 - \beta^2 \sin^2 \psi)^{3/2}}, \quad (6)$$

where ψ is the angle between the projectile velocity and the radial vector to a particle in the target, and the usual relativistic variables are

$$\beta = \frac{v}{c}, \quad (7)$$

$$\gamma = (1 - \beta^2)^{-1/2}. \quad (8)$$

The incorporation of these relativistic fields reduces the longitudinal range of interaction with the projectile and increases the magnitude of the transverse field [10].

III. RESULTS AND DISCUSSION

A. Transverse electron-electron correlation

To investigate ion-molecule collisions, the final-state electron momenta for the double-ionization reactions $\text{Se}^{28+} + \text{H}_2$ at 3.6 MeV/u ($v_p = 12.0$ a.u.) and $\text{U}^{92+} + \text{H}_2$ at 1 GeV/u ($\beta = v_p/c = 0.88$) have been studied. The final-state momentum components are rotated into a Cartesian coordinate system where the unit vectors are defined as $\hat{\mathbf{p}}_{\parallel}$ in the direction of the initial projectile momentum, $\hat{\mathbf{p}}_x$ in the direction of the final transverse component of the center of mass of the two recoiling and exploding H^+ ions, and $\hat{\mathbf{p}}_y$ is chosen to construct a right-hand coordinate system.

To observe the correlation between the electrons, a component of one electron's final momentum is plotted versus the same component of the second electron. Similar plots have previously been used by Moshhammer *et al.* [4] and Wood *et al.* [10] to display electron correlation in longitudinal spectra. By displaying the spectra in this fashion, one can see in each dimension how the electrons and possibly other particles are interacting. An absence of correlation would be noted by the lack of a distinct pattern in the spectra. The additional use of the rotation into the collision coordinate system allows one to see detailed momentum balance along with the electron-electron correlation.

The $\text{Se}^{28+} + \text{H}_2$ double-ionization longitudinal spectrum for the electrons is presented at the top of Fig. 2, with $P_{e1\parallel}$ along the horizontal axis and $P_{e2\parallel}$ along the vertical axis. This is equivalent to plotting the sum momentum of the electrons, $P_{e1\parallel} + P_{e2\parallel}$, versus relative momentum, $P_{e2\parallel} - P_{e1\parallel}$, if the coordinate system is rotated by 45° clockwise. From this figure it is clear that both electrons are ejected with forward longitudinal momentum. This is due to the long postcollision interaction with the projectile. The majority of double-ionization events lead to both electrons having small $P_{e\parallel}$, without a strongly observed correlation. However, on the edges of the distribution a pattern is noticed where one electron is fast in the longitudinal direction while the other electron is slow. This pattern is the result of including the electron-electron interaction in the postcollision regime, and it is not observed when this interaction is absent [4].

Because the peak in the longitudinal plot does not show strong correlation effects does not imply that most collisions result in noncorrelated electrons. We find the correlation is more apparent in the transverse plane where the long postcollision interaction of the electrons with the highly charged projectile ion is minimized. By making use of the collision

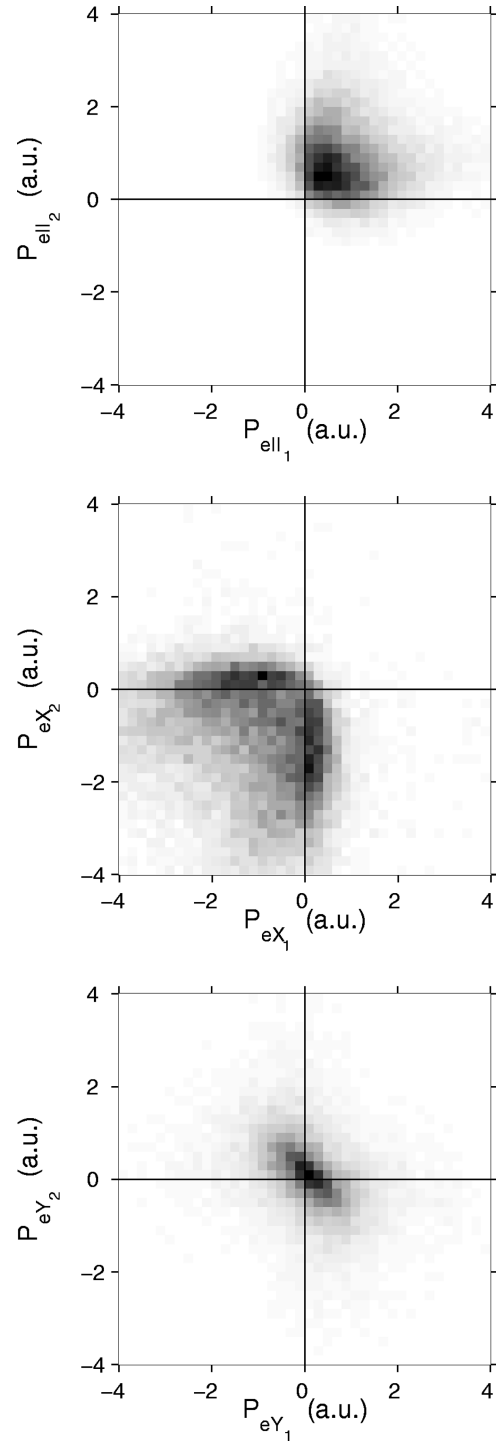


FIG. 2. Calculated correlation of the electron spectra for 3.6-MeV/u $\text{Se}^{28+} + \text{H}_2$. Top: $P_{e1\parallel}$ vs $P_{e2\parallel}$; middle: P_{e1x} vs P_{e2x} ; bottom: P_{e1y} vs P_{e2y} . Each plot is on a linear scale, with darker areas representing a higher cross section.

plane with the transverse recoil-ion momentum defining the p_x coordinate, $P_{R\perp} = P_{Rx}$, an interesting correlation is apparent. In the middle of Fig. 2 is a plot of P_{e1x} versus P_{e2x} . The p_x component of electron momentum is parallel or antiparallel to the transverse recoil momentum. For both axes, $P_{R\perp}$ is along the positive portion of the axis (P_{Rx} is always positive). For example, any density in the first quadrant would signify that both electrons and the recoil ion each have posi-

tive components of momentum in the p_x direction. The $P_{e_{1x}}$ versus $P_{e_{1x}}$ spectrum of Fig. 2 clearly portrays the electron correlation and also momentum balance. The event spectrum shows that one electron is ejected opposite the center of mass of the recoil ions with a broad range of P_e . The other electron is apparently constrained to small values of positive P_{ex} . In the case of independent electrons, it would be expected that both electrons be ejected with p_x opposite that of the recoil. In our calculation the electrons are not independent, so the electrons will repel each other. It is unlikely that an electron will be observed with a large value of P_{ex} in this direction, since the transverse momentum of the recoil ion accounts for most of the momentum in this direction. A large positive P_{ex} can occur when the projectile is scattered strongly off the target.

The lower portion of Fig. 2 is a plot of $P_{e_{1y}}$ versus $P_{e_{2y}}$. This plot is interesting since momentum in the p_y direction is carried mainly by the electrons. The recoil has a zero component of P_{Ry} , and the projectile's transverse momentum is normally opposite the recoil. Two-body momentum balance and electron correlation then lead to the back-to-back pattern observed in the lower section of Fig. 2. The tendency for one electron to be fast and the other slow is also noticed in the outer regions in this direction.

Calculations for double ionization of H_2 by relativistic 1-GeV/u U^{92+} ions have also been carried out, and the results are displayed in Fig. 3 in the same fashion as above. For the longitudinal case, the pattern is changed considerably from the 3.6-MeV/u Se^{28+} case, with the distribution being centered at the origin. The shift toward the center is due to lack of postcollision interaction from the projectile due to relativistic reduction of the longitudinal impulse given to the ionized electron by the projectile. The pattern for the p_x direction is similar to the previous case, but a significant number of events are observed with both electrons having positive values of $P_{e\parallel}$. These reactions probably occur when the projectile is strongly scattered by the target. The recoil ion and electrons balance the momentum transfer by moving in the $+p_x$ direction, and the electron correlation is in the p_y or p_z direction. It is also possible that the recoil ions have a very small transverse momentum, due to scattering mainly between the electrons and the projectile. A decrease in the transverse correlation will also occur because the lack of PCI with the projectile increases the longitudinal correlation. Looking at the p_y direction, the pattern is broader along the $P_{e_{2y}}-P_{e_{1y}}$ diagonal. This indicates the projectile is playing more of a role in momentum balance in this direction than in the 3.6-MeV/u Se^{28+} system.

B. Orientation effects

To explore the double electron removal dependence on the orientation of the molecular axis, calculations for $O^{8+}+H_2$ at 500 keV/u have been made. Double electron removal at 500 keV/u includes both the double-ionization and transfer-ionization processes. To determine the orientation dependence, the angle of the final-state momentum of the dissociation products (H^+) with the incident beam direction is determined. This is in accordance with experimental methods, and assumes that the rotation of the molecule is much

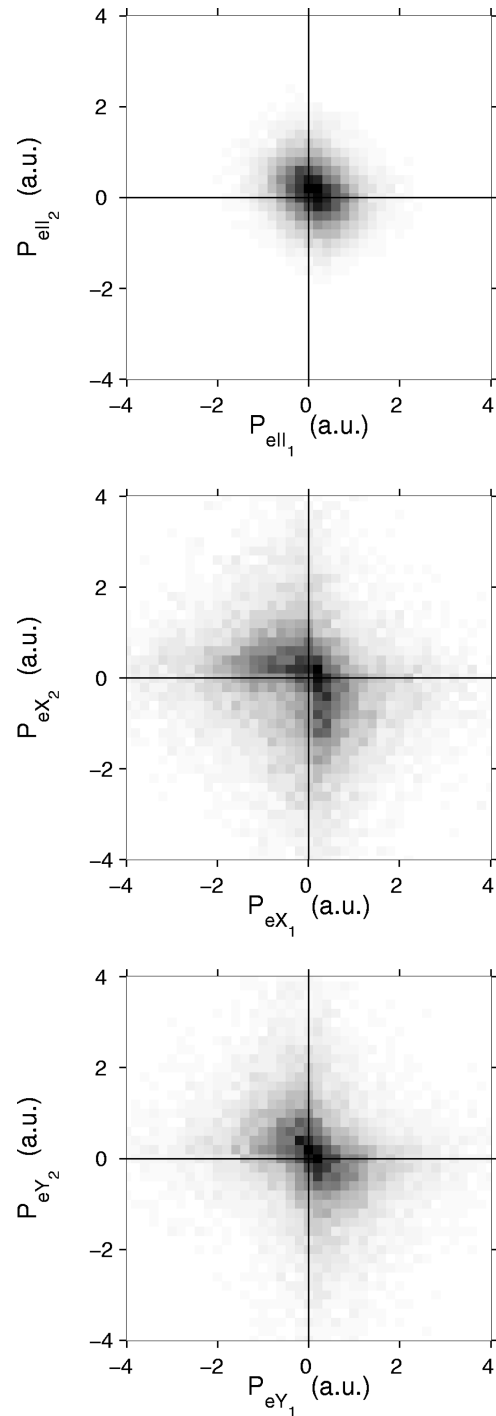


FIG. 3. Calculated correlation of the electron spectra for 1-GeV/u $U^{92+} + H_2$. Top: $P_{e_{1\parallel}}$ vs $P_{e_{2\parallel}}$; middle: $P_{e_{1x}}$ vs $P_{e_{2x}}$; bottom: $P_{e_{1y}}$ vs $P_{e_{2y}}$. Each plot is on a linear scale, with darker areas representing a higher cross section.

slower than the collision time. The single differential $d\sigma/d \cos \theta$ is plotted as a function of θ , the polar angle of a H^+ ion. The double-ionization results are shown in Fig. 4. No dependence on the orientation has been found for this case, in agreement with the measurements and conclusions of Cheng *et al.* [14]. The experimental data shown in Fig. 4 have been normalized to the calculations. The experiment included both double-ionization and ionization excitation processes because the different channels could not be distin-

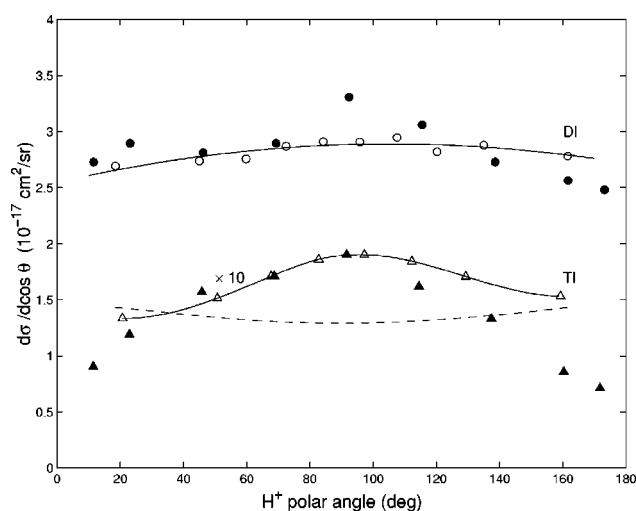


FIG. 4. Angular distributions $d\sigma/d \cos \theta$ of the target H^+ ions for double and transfer ionization by 500-keV/u O^{8+} . Open circles—CTMC double-ionization results, full circles—Cheng *et al.* [14]. Open triangles—CTMC transfer-ionization results, full triangles—Cheng *et al.* [14], dashed line—transfer-ionization calculations without the inclusion of electron-electron and electron-other-target-nucleus interactions.

guished in the study, while the calculation in Fig. 4 is limited to double ionization. The cross section lacks orientation dependence because the range of interaction for double electron removal of approximately 5 a.u. greatly exceeds the internuclear separation of H_2 .

On the other hand, the range of interaction for transfer ionization is smaller than that for double ionization. The calculated distribution for transfer ionization in Fig. 4 is not isotropic, but has a peak value at 90° about 1.5 times the minimum located at 0° . This is consistent with the observed data of Cheng *et al.* [14] for the same system. A slight asymmetry is noticed in the spectrum of the CTMC calculations. The distribution has a slightly higher magnitude at 180° than at 0° since the $H^+ + H^+$ center of mass is found in the backward direction.

The transfer-ionization results are surprising for two reasons. First, one would expect more transfer ionization to occur when the H_2 internuclear axis is parallel to the incident beam since the electron capture mechanism, unlike the ionization process, is of short range. The O^{8+} projectile moving parallel to the axis could independently capture one electron and ionize the other as it passes the molecule. This is not observed, however, as the maximum of the distribution is found at 90° . Second, the anisotropy in the distribution has been attributed to interference between the atomic centers [14,17]. A quantal interference effect is certainly not possible in our classical calculation. It should be noted that the experimentally observed height of the maximum above the minimum is appreciably higher than the height found in the present calculations. Also, note that when the calculations did not include the electron-electron and electron-other-target-nuclei interactions, the anisotropy was reversed with a minimum at 90° rather than a maximum.

Thus our calculations with and without all interactions substantiate that dynamical electron-electron or electron-other-target-nucleus correlations play a role in the anisotropy

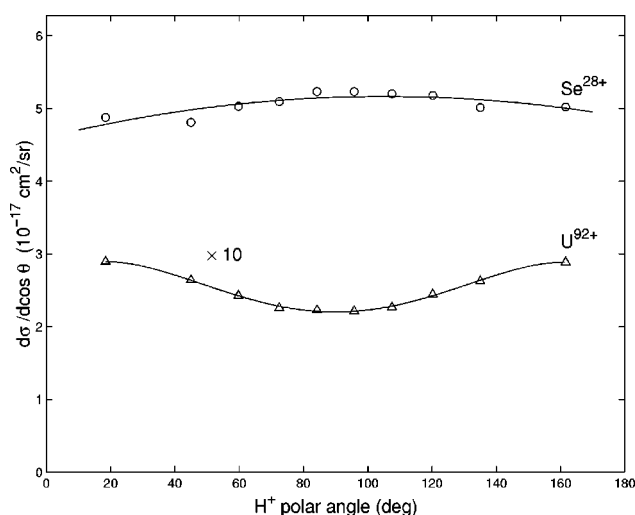


FIG. 5. Angular distributions $d\sigma/d \cos \theta$ of H^+ ions for double ionization of H_2 by 3.6-MeV/u Se^{28+} and 1-GeV/u U^{92+} .

due to the orientation of the molecular axis. For example, the first ionized electron could subsequently ionize the second electron through the Thomas electron-electron scattering process investigated by Mergel *et al.* [27]. A more probable explanation is that the conventional electron-nuclear Thomas mechanism increases the capture probability for molecules aligned perpendicular to the projectile velocity, giving rise to a maximum for alignments of 90° . In this case, a hard collision of one electron with the projectile scatters the electron around the other proton nucleus to be captured by the projectile via a process similar to that for Thomas scattering in an atom. Such an explanation would be consistent with that given by quantal calculations in that second-order processes, such as scattering from the second nucleus, are required to explain the experimental observations.

The orientation dependence for other systems, namely, 3.6-MeV/u $Se^{28+} + H_2$ and 1-GeV/u $U^{92+} + H_2$, have also been examined, Fig. 5. The double electron removal mechanism for these fast collisions is double ionization, so it can be determined if increasing the projectile velocity changes the orientation dependence of the double-ionization cross section. Experimental measurements [14] of $O^{8+} + H_2$ indicate that the $d\sigma/d \cos \theta$ distribution remains isotropic up to 1 MeV/u. The CTMC calculations at a higher impact energy of 3.6-MeV/u $Se^{28+} + H_2$ are also isotropic, as seen in Fig. 5. The results are quite different for 1-GeV/u $U^{92+} + H_2$, Fig. 5, as a minimum is found at 90° . The lower probability of double ionization at 90° for this very fast collision is attributed to the short range of interaction and the low energy of the ejected electrons. The impact parameter range of interaction for double ionization of the 500-keV/u and 3.6-MeV/u collisions is about three times the size of the hydrogen molecule, essentially making the H_2 look like a two-electron atom. In the 1-GeV/u case, most double-ionization events occur within an impact parameter about the size of the molecule. An orientation 90° to the beam decreases the chance of the projectile closely approaching both electrons, and thus decreases the probability of sequential ionization. In addition, at 1-GeV/u, electrons are ejected with low energy and perpendicular to the beam direction [10]. The possibility exists for double scattering, however, the low energy of the

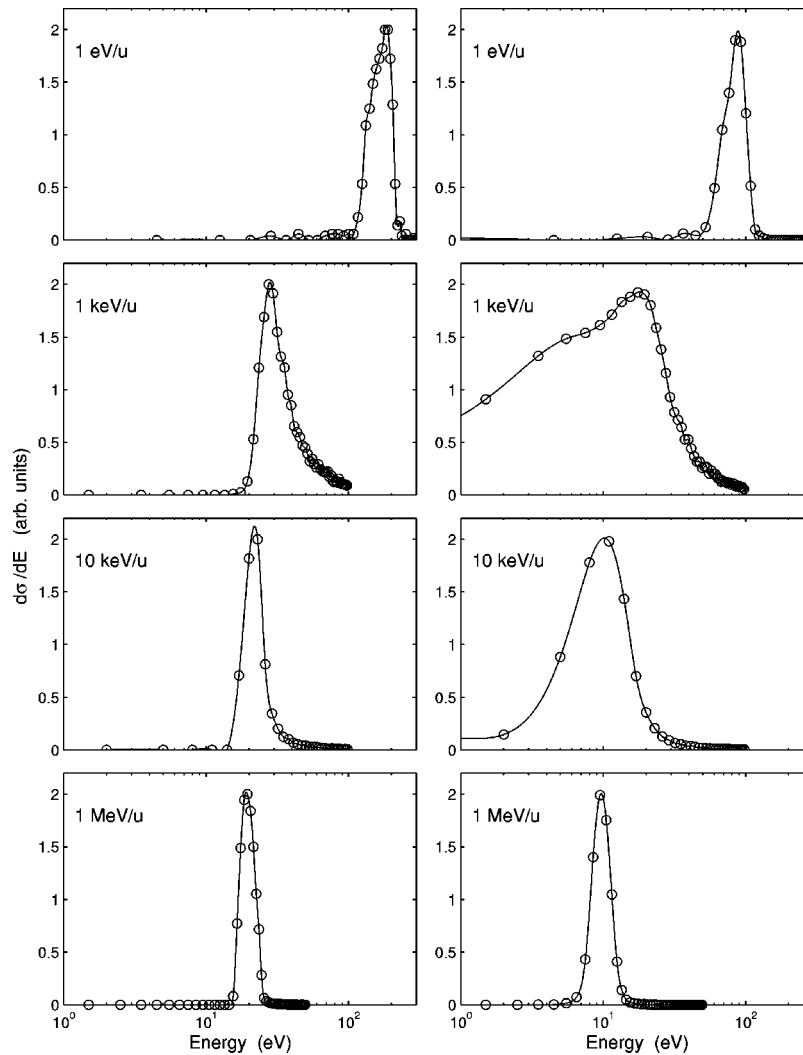


FIG. 6. Energies of the protons after double electron removal by Xe^{54+} . The left-hand side represents the total energy of both ions, and the right-hand side represents energies of a single ion.

ejected electrons makes an ionization from an electron-electron interaction improbable.

C. $\text{Xe}^{54+} + \text{H}_2$ double electron removal: Fragmentation of H_2

The removal of both electrons from the hydrogen molecule results in a Coulomb explosion between the target protons and the projectile. To investigate the properties of the energy and momentum spectra of the protons, simulations of the collision system $\text{Xe}^{54+} + \text{H}_2$ at impact energies of 1 eV/u, 1 keV/u, 10 keV/u, and 1 MeV/u have been made. The low energy of 1 eV/u was chosen to test calculated capture cross sections versus measurements from the Livermore EBIT facility by Beck *et al.* [19]. These experiments were performed for a collision system with a center-of-mass energy of 6 eV. A linear fit to the measurements by these workers provides a total capture cross section of $12 \times 10^{-14} \text{ cm}^2$ for a projectile charge of $q=54$. In comparison, the CTMC calculations predict a total cross section of $5.1 \times 10^{-14} \text{ cm}^2$. Our calculations are within the error bars of the measurement, where absolute values were obtained by normalizing to experiments by Kravis *et al.* [28]. Moreover, the measurements by Kravis *et al.* are consistently a factor of about 2 above those of Can *et al.* [29], to which we compare well. The ratio of the

double capture to the total cross section, σ_D/σ_T , was calculated to be 57%, while the EBIT researchers observed a nearly constant value of about 30% for projectiles with $q \geq 35$. The large difference is most likely due to neglecting Auger decay of the captured electrons in our model. The predictions include events that may eventually Auger decay and result in transfer ionization, not double electron capture.

The removal of two electrons from H_2 automatically leads to the dissociation of the molecule and two free H^+ ions. The kinetic energy of the two ions in the final state has two sources: the energy transferred from the projectile during the collision, and the energy from the Coulomb repulsion between the protons. The energy spectra of the dissociation products are shown in Fig. 6 for Xe^{54+} impact over a broad range of impact energies. At the lowest energies double electron capture is the dominant collision mechanism with capture proceeding into a narrow band of n levels around $n=18$. At the higher energies, impact ionization of both electrons is the main double electron removal mechanism.

The left-hand side of Fig. 6 is the distribution for the sum of the energies of both H^+ ions, and the right-hand side is the energy distribution for individual H^+ ions. The figure shows that the total energy sum of the two ions increases as the

collision energy decreases. The high energy protons produced from impact at 1 eV/u are due to a large collisional transfer of energy to the target from the projectile. In essence this is a three-body Coulomb explosion between the positively charged heavy ions since the collision time is quite extended. The extent of the Coulomb explosion is not as large as given by the simple ratio of the projectile to proton charges, since in these slow collisions the impact parameter range is extended to almost 40 a.u. As the impact energy increases and the collision time decreases, less energy is collisionally transferred to the target and the total energy approaches the Franck-Condon transition energy of the isolated molecule, ~ 19 eV. At 1 keV/u the distribution for the total proton energy peaks around 30 eV, with 10 eV from transfer during the collision, and 20 eV from dissociation. At 10 keV/u and 1 MeV/u the amount of energy obtained from the collision is very small, and the positions of the peaks approach the isolated molecule Franck-Condon limit.

When the energies of the individual ions are examined, the right side of Fig. 6, a consistent trend is noticed. Below ~ 10 keV/u, appreciable deviations from Franck-Condon behavior appear. Such deviations are consistent with the non-Franck-Condon behavior observed by Giese *et al.* [30] for ~ 20 -eV/u $\text{Ar}^{5+} + \text{H}_2$ collisions. At 1 eV/u the distribution indicates that the energy transferred to the ions is nearly equal, with each proton absorbing half of the collisional energy. However, at 1 keV/u the energy distribution for the individual ions is much wider than that for the total energy. The protons do not equally share the available energy, as is evident by the number of low energy ions. This is also apparent, but not as extreme, at 10 keV/u. At 1 MeV/u, the distribution peaks at about 10 eV, indicating that the ions equally share the 19 eV of energy liberated in the explosion of the molecule. To explain the process at 1 and 10 keV/u, the right side of Fig. 6 must be closely examined. The energy transferred to the center of mass of the ions by the 1-keV/u Xe^{54+} is about 10 eV. When the ions equally share the 20 eV from the dissociation, each will have 10 eV of energy. If the Coulomb explosion directs an H^+ opposite the center-of-mass motion (determined by the collision with the projectile), a low energy proton in the laboratory frame will be the result.

To further explore this effect, the energy of one H^+ is plotted versus the energy of the other H^+ in Fig. 7. At low energy the projectile transfers about equal amounts of energy to each H^+ , so the $E_{\text{H}^+}^1 = E_{\text{H}^+}^2$ line is dense and the Franck-Condon energies from the breakup are folded into the pattern. At high impact energies, in the lower plot of Fig. 7, the energy is from the target Coulomb explosion, so the density is concentrated around $E_{\text{H}^+}^1 = E_{\text{H}^+}^2 = 10$ eV. The pattern for 1-keV/u Xe^{54+} impact is markedly different from the others. The dominant feature in this case is the one-fast-one-slow distribution of the energies. This is again due to collisional energy being about the same as the dissociation energy.

If the longitudinal momentum of the exploding protons is examined, more features of the dynamics can be seen, as presented in Fig. 8. At 1 eV/u, the spectrum is pushed forward by the incoming slow Xe^{54+} projectile. A minimum is found near zero, and a smaller peak is found in the backward direction. The width of the distribution demonstrates the

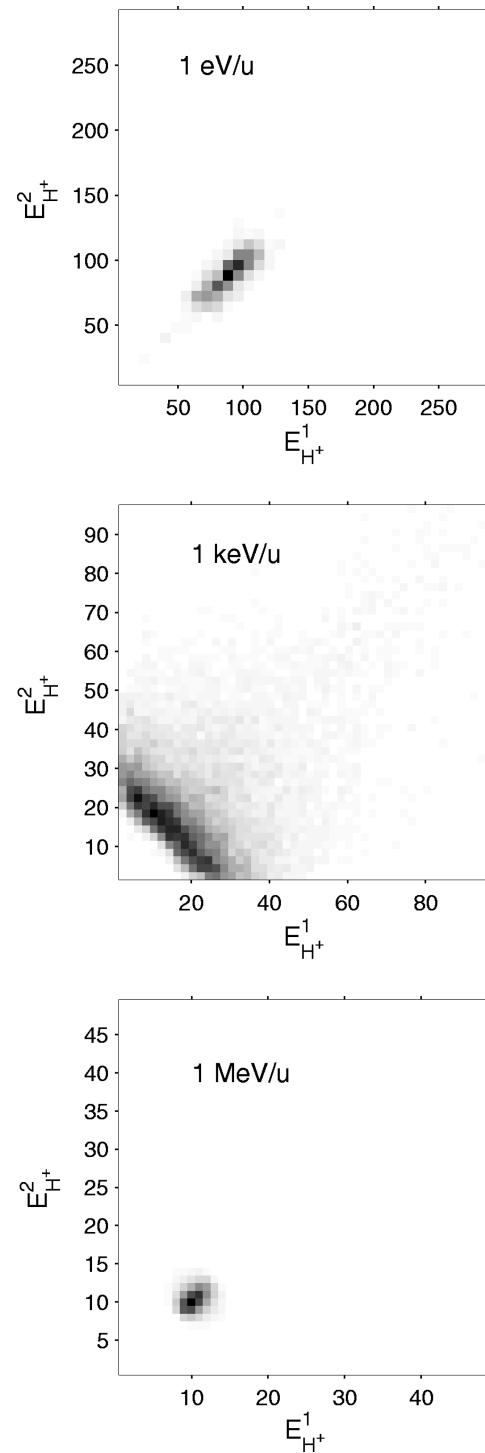


FIG. 7. The energy sharing, $E_{\text{H}^+}^1$ vs $E_{\text{H}^+}^2$, between the H^+ ions for double electron removal by 1-eV/u Xe^{54+} (top), 1-keV/u Xe^{54+} (middle), 1-MeV/u Xe^{54+} (bottom).

large momentum transfer from the collision. The 1-keV/u spectrum of Fig. 8 is antisymmetric about $p_{\parallel}=0$, with the distribution showing more ions moving with negative p_{\parallel} . At 1 MeV/u, in the bottom of Fig. 8, the longitudinal momentum spectrum is symmetric about the origin and is flat on the top. This is expected because of the small momentum transfer during the collision.

It is of interest to further study the momentum of the dissociation products in a coordinate frame similar to that

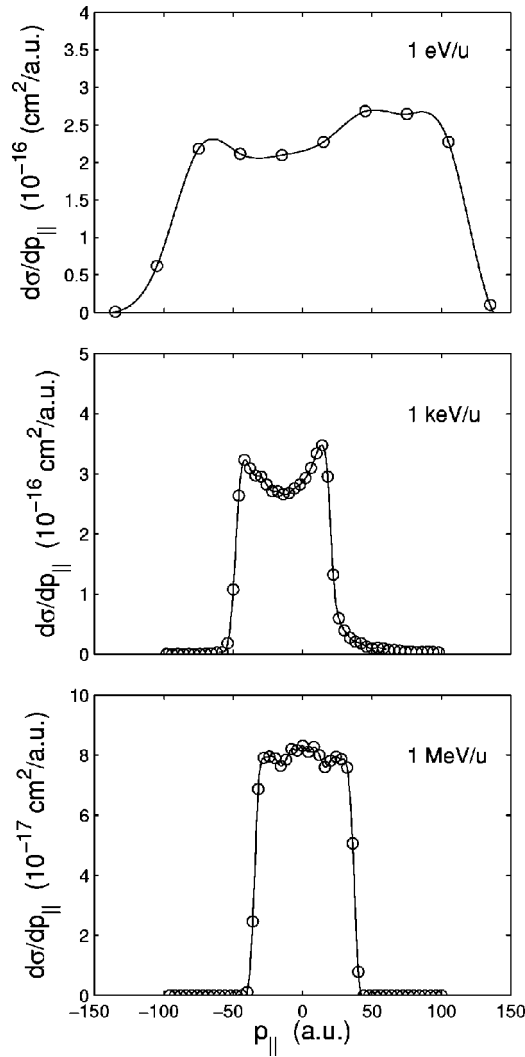


FIG. 8. Longitudinal momentum spectra of H^+ ions after double electron removal by Xe^{54+} at impact energies of: top, 1 eV/u; middle, 1 keV/u; bottom, 1 MeV/u.

already used to study electron correlation. In this case, however, the p_x component is defined by the final transverse component of the projectile momentum. In Fig. 9 the momentum of the protons is plotted for Xe^{54+} impact at 1 eV/u. The top plot shows $p_{||}$ on the horizontal axis and p_x on the vertical axis. The projectile's transverse momentum is in the positive p_x direction. From this plot one can see that the protons and the Xe^{54+} projectile scatter in opposite directions from one another. The semicircular pattern of the proton spectra demonstrates how the momentum is distributed to give the energy spectra of Fig. 6. The middle portion of Fig. 9 is a plot of $p_{||}$ versus p_y . The pattern here shows no structure or correlation. The p_y component is of less importance here because large impact parameters of the collision result in relatively small transverse momentum components perpendicular to the line between the projectile and the target center. In the lower plot of Fig. 9 the p_x components of the protons are plotted against each other. The main density here is at $\sim(-100, 100)$ a.u. The interaction with the highly charged projectile clearly dominates over the H^+-H^+ interaction in this collision.

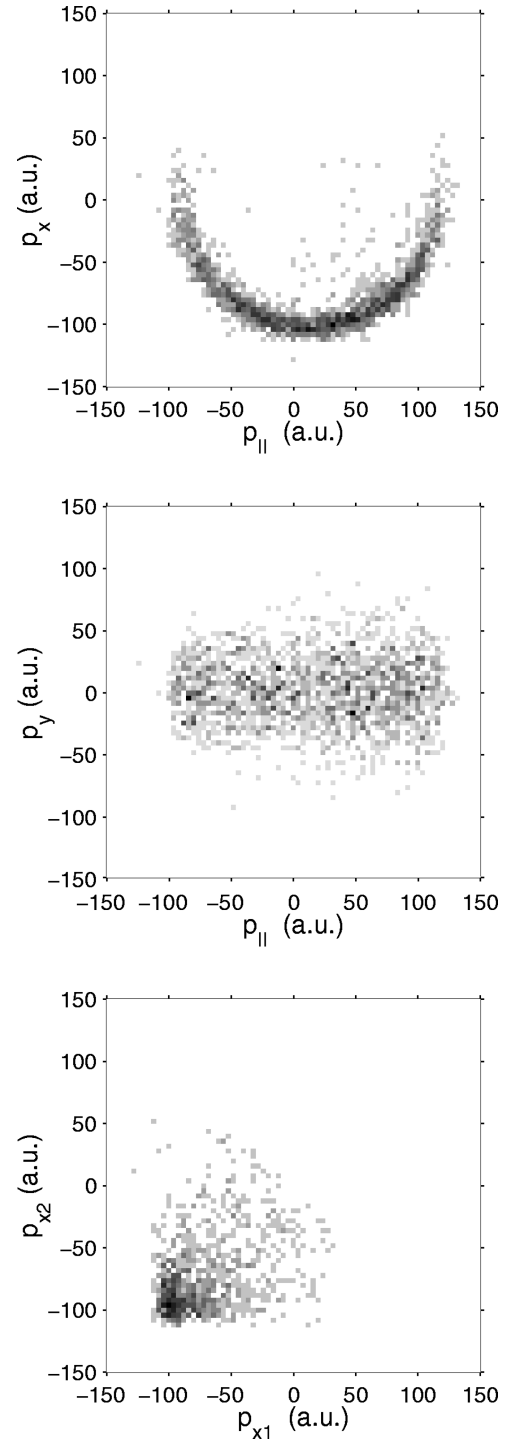


FIG. 9. 1-eV/u $Xe^{54+} + H_2$ momentum spectra of the dissociated protons. Top: $p_{||}$ vs p_x ; middle: $p_{||}$ vs p_y ; bottom: p_{x1} vs p_{x2} . The transverse projectile momentum is along $+p_x$.

At 1 keV/u, the collisional energy transfer is about the same as the energy released in the molecular breakup. The $p_{||}$ versus p_x plot on the top has a circular pattern centered around $p_{||} \approx -10$ and $p_x \approx -10$ a.u. The shift from the origin is due to the collisional interaction with the projectile. The dark high density areas show the protons moving opposite the projectile in the transverse direction. Many protons are found outside of the spherical momentum shell, and these protons have excess momentum in the negative p_x direction. These are the protons that cause the broad energy distribu-

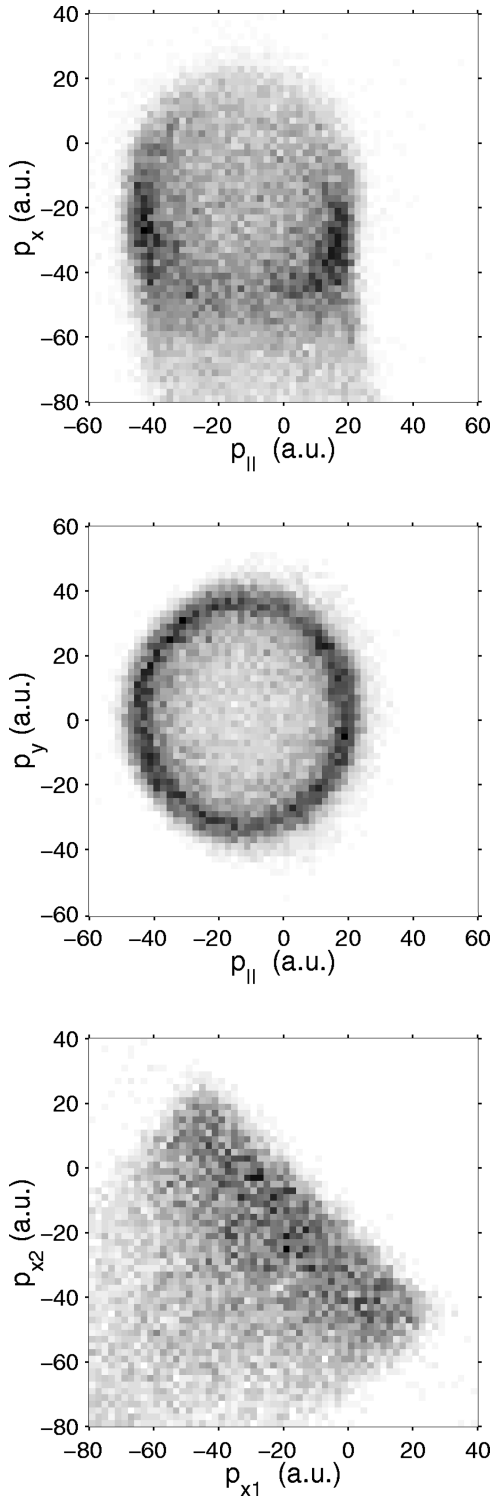


FIG. 10. 1-keV/u $\text{Xe}^{54+} + \text{H}_2$ momentum spectra of the dissociated protons. Top: p_{\parallel} vs p_x ; middle: p_{\parallel} vs p_y ; bottom: p_{x1} vs p_{x2} . The transverse projectile momentum is along $+p_x$.

tion in the 1-keV/u plot of the individual protons in Fig. 6. In the middle part of Fig. 10 the p_{\parallel} versus p_y distribution is a circular pattern with maxima at the edge of the circle. The distribution is pushed back in the longitudinal direction and is symmetric about $p_y=0$. The protons balance each other exactly in this plane because the projectile transverse momentum (including the captured electrons) is in the p_x direction. The momentum in this plane is a combination of the

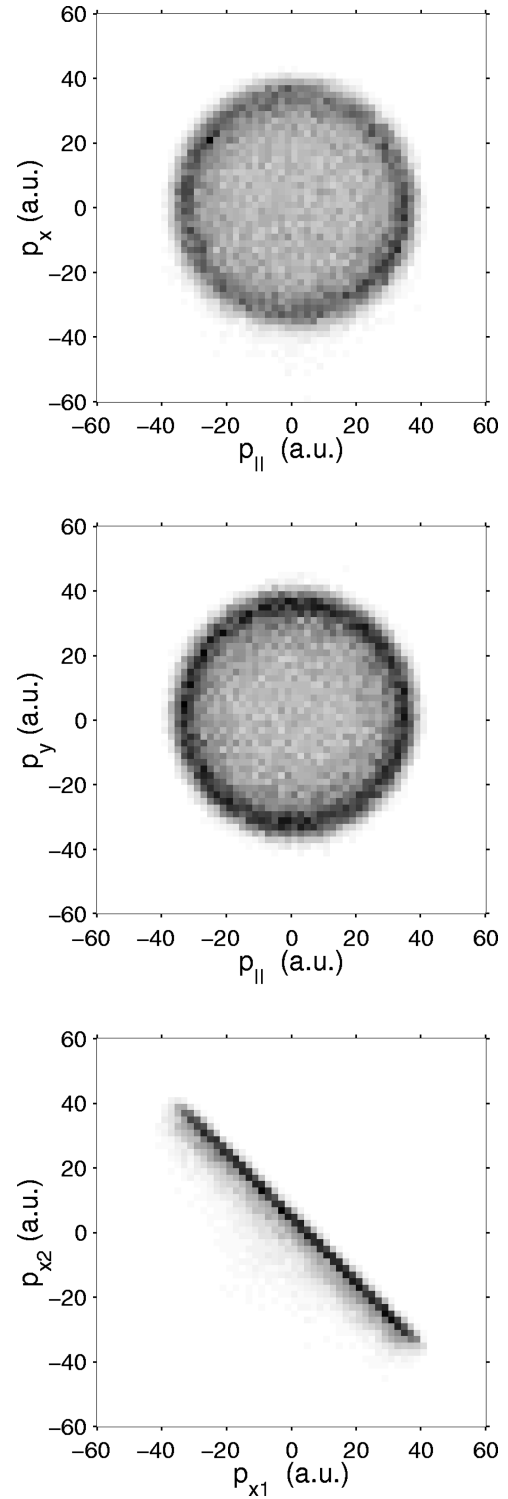


FIG. 11. 1-MeV/u $\text{Xe}^{54+} + \text{H}_2$ momentum spectra of the dissociated protons. Top: p_{\parallel} vs p_x ; middle: p_{\parallel} vs p_y ; bottom: p_{x1} vs p_{x2} . The transverse projectile momentum is along $+p_x$.

collisional and breakup interactions. A plot of p_{x1} versus p_{x2} in the lower part of Fig. 10 shows back-to-back ($p_{x1} = -p_{x2}$) motion, but the collisional transfer to the center of mass of the target spreads the event distribution. Note that close collisions with a small impact parameter may force both protons to have large and negative values of p_x .

For the 1-MeV/u $\text{Xe}^{54+} + \text{H}_2$ fast collision, the dissociating protons behave as expected for a Franck-Condon transi-

tion. Only small energy and momentum transfers occur, so the momentum given to the protons during the breakup is clearly seen. In Fig. 11, the p_x versus p_{\parallel} and p_y versus p_{\parallel} are symmetric about the origin. A three-dimensional picture would be a thin spherical surface of radius $p = \sqrt{2mE}$ in momentum space. Back-to-back proton emission is observed for p_{x1} versus p_{x2} , as would be expected in this case where the projectile deposits its energy and then recedes and is very distant when the two protons commence their breakup.

IV. CONCLUSIONS

Five-body classical trajectory Monte Carlo calculations have been presented for double electron removal from molecular hydrogen. Correlation between the ejected electrons has been observed in the double ionization of H_2 by 3.6-MeV/u Se^{28+} and 1-GeV/u U^{92+} . The correlation is found in both the longitudinal and transverse directions. Our results show the importance of the postcollision interactions between the electrons and recoil and projectile ions. However, the lack of initial-state correlation limits the completeness of the theory.

The dependence of cross sections on the alignment of the molecular axis was determined for transfer ionization and double ionization. The absence of any dependence for double ionization at intermediate energies is in agreement with experiment. The prediction for the minimum at 90° for relativistic U^{92+} projectiles has yet to be confirmed by experiment. The maximum found at 90° for transfer ionization in 500-keV/u $O^{8+} + H_2$ was surprising, since it has commonly been attributed to interference between the atomic centers. We found that such a peak only occurs for calculations where the

electron-electron and electron-other-proton-nucleus interactions are included in the description of the collision. Such an observation indicates that the Thomas double scattering mechanism, where the electron from one center scatters from the other target center, preferentially proceeds when the molecular axis is perpendicular to the projectile velocity. When these latter interactions were not included in the calculations, a minimum, rather than a maximum, was obtained at 90° .

Examination of the proton energies after double electron removal reactions resulted in the observation of differing energy sharing behavior. At low collision energy the interaction with the projectile produced very "hot" protons due to the Coulomb explosion of the protons against the highly charged projectile ion during the slow collision. In contrast, at high collision energies, we found the usual Franck-Condon breakup pattern because the projectile was absent from the target region during the dissociation process. However, in intermediate to slow collisions such as 1- to 10-keV/u Xe^{54+} , the collisional energy transfer is comparable to the energy at the Franck-Condon limit. Here, we found both "hot" and "slow" protons. We did not expect the presence of slow protons, which resulted in lengthy checks of the computer code. If such a prediction is confirmed experimentally, it may be possible that unique slow dissociation products can be produced by collisions of highly charged ions with molecules at intermediate energies around 1–10 keV/u.

ACKNOWLEDGMENT

This work was supported by the Department of Energy, Office of Fusion Energy Sciences.

-
- [1] J. Ullrich, R. Moshhammer, R. Dörner, O. Jagutzki, V. Mergel, H. Schmidt-Böcking, and L. Spielberger, *J. Phys. B* **30**, 2917 (1997).
 - [2] R. Moshhammer, J. Ullrich, M. Unverzagt, W. Schmidt, P. Jardin, R. E. Olson, R. Mann, R. Dörner, V. Mergel, U. Buck, and H. Schmidt-Böcking, *Phys. Rev. Lett.* **73**, 3371 (1994).
 - [3] R. Moshhammer, M. Unverzagt, W. Schmidt, J. Ullrich, and H. Schmidt-Böcking, *Nucl. Instrum. Methods Phys. Res. B* **108**, 425 (1996).
 - [4] R. Moshhammer, J. Ullrich, H. Kollmus, W. Schmitt, M. Unverzagt, O. Jagutzki, V. Mergel, H. Schmidt-Böcking, R. Mann, C. J. Wood, and R. E. Olson, *Phys. Rev. Lett.* **77**, 1242 (1996).
 - [5] R. Moshhammer, J. Ullrich, H. Kollmus, W. Schmitt, M. Unverzagt, H. Schmidt-Böcking, C. J. Wood, and R. E. Olson, *Phys. Rev. A* **56**, 1351 (1997).
 - [6] R. E. Olson, C. J. Wood, H. Schmidt-Böcking, R. Moshhammer, and J. Ullrich, *Phys. Rev. A* **58**, 270 (1998).
 - [7] C. J. Wood, C. R. Feeler, and R. E. Olson, *Phys. Rev. A* **56**, 3701 (1997).
 - [8] R. Dörner, H. Khemliche, M. H. Prior, C. L. Cocke, J. A. Gary, R. E. Olson, V. Mergel, J. Ullrich, and H. Schmidt-Böcking, *Phys. Rev. Lett.* **77**, 4520 (1996).
 - [9] S. D. Kravis, M. Abdallah, C. L. Cocke, C. D. Lin, M. Stockli, B. Walch, and Y. D. Wang, *Phys. Rev. A* **54**, 1394 (1996).
 - [10] C. J. Wood, R. E. Olson, W. Schmitt, R. Moshhammer, and J. Ullrich, *Phys. Rev. A* **56**, 3746 (1997).
 - [11] S. Keller, H. J. Lüdde, and R. M. Dreizler, *Phys. Rev. A* **55**, 4215 (1997).
 - [12] U. Werner, N. M. Kabachnik, V. N. Kondratyev, and H. O. Lutz, *Phys. Rev. Lett.* **79**, 1662 (1997).
 - [13] G. Sampoll, R. L. Watson, O. Heber, V. Horvat, K. Wohrer, and M. Chabot, *Phys. Rev. A* **45**, 2903 (1992).
 - [14] S. Cheng, C. L. Cocke, V. Frohne, E. Y. Kamber, J. H. McGuire, and Y. Wang, *Phys. Rev. A* **47**, 3923 (1993).
 - [15] R. L. Ezell, A. K. Edwards, R. M. Woods, M. W. Dittman, J. F. Browning, and M. A. Mangan, *Nucl. Instrum. Methods Phys. Res. B* **56/57**, 292 (1991).
 - [16] A. K. Edwards, R. M. Wood, M. A. Mangan, and R. L. Ezell, *Phys. Rev. A* **46**, 6970 (1992).
 - [17] H. F. Busnengo, S. E. Corchs, R. D. Rivarola, and J. H. McGuire, *Nucl. Instrum. Methods Phys. Res. B* **98**, 227 (1995).
 - [18] K. Wohrer and R. L. Watson, *Phys. Rev. A* **48**, 4784 (1993).
 - [19] B. R. Beck, J. Steiger, G. Weinberg, D. A. Church, J. McDonald, and D. Schneider, *Phys. Rev. Lett.* **77**, 1735 (1996).
 - [20] L. M. Wiese, O. Yenen, B. Thaden, and D. H. Jaacks, *Phys. Rev. Lett.* **79**, 4982 (1997).

- [21] R. Abrines and I. C. Percival, Proc. Phys. Soc. London **88**, 861 (1966).
- [22] R. E. Olson and A. Salop, Phys. Rev. A **16**, 531 (1977).
- [23] C. O. Reinhold and C. A. Falcon, Phys. Rev. A **33**, 3859 (1986).
- [24] V. J. Montemayor and G. Schiwietz, Phys. Rev. A **40**, 6223 (1989).
- [25] L. Meng, C. O. Reinhold, and R. E. Olson, Phys. Rev. A **40**, 3637 (1989).
- [26] G. Herzberg, *Molecular Spectra and Molecular Structure I. Spectra of Diatomic Molecules* (Van Nostrand, New York, 1939).
- [27] V. Mergel *et al.*, Phys. Rev. Lett. **79**, 387 (1997).
- [28] S. Kravis, H. Saitoh, K. Okuno, K. Soejima, M. Kimura, I. Shimamura, Y. Awaya, Y. Kaneko, M. Oura, and N. Shimakura, Phys. Rev. A **52**, 1206 (1995).
- [29] C. Can, T. Gray, S. L. Varghese, J. M. Hall, and L. N. Tunnel, Phys. Rev. A **31**, 72 (1984).
- [30] J. P. Giese, C. L. Cocke, W. T. Waggoner, J. O. K. Pedersen, E. Y. Kamber, and L. N. Tunnell, Phys. Rev. A **38**, 4494 (1988).